

# High temporal resolution modelling of environmentally-dependent seabird ammonia emissions: Description and testing of the GUANO model



S.N. Riddick<sup>a, b, c, \*</sup>, T.D. Blackall<sup>b</sup>, U. Dragosits<sup>a</sup>, Y.S. Tang<sup>a</sup>, A. Moring<sup>a, e</sup>, F. Daunt<sup>a</sup>, S. Wanless<sup>a</sup>, K.C. Hamer<sup>d</sup>, M.A. Sutton<sup>a</sup>

<sup>a</sup> Centre for Ecology & Hydrology Edinburgh, Bush Estate, Penicuik, Midlothian, EH26 0QB, UK

<sup>b</sup> Department of Geography, King's College London, Strand, London, WC2R 2LS, UK

<sup>c</sup> Department of Civil and Environmental Engineering, Princeton University, Princeton, 08540, USA

<sup>d</sup> School of Biology, University of Leeds, Leeds, LS2 9JT, UK

<sup>e</sup> School of Geosciences, University of Edinburgh, EH9 3FE, UK

## HIGHLIGHTS

- A dynamic mass-flow model to simulate variation in NH<sub>3</sub> emissions from seabird guano.
- Model output validated against measurements from colonies across a range of climates.
- Model output captures observed dependence of NH<sub>3</sub> emission on environmental variables.
- This model can be a starting point to model NH<sub>3</sub> emissions from other sources.

## ARTICLE INFO

### Article history:

Received 5 December 2016

Received in revised form

29 March 2017

Accepted 12 April 2017

Available online 15 April 2017

### Keywords:

Seabird

Ammonia

Dynamic model

Climate

## ABSTRACT

Many studies in recent years have highlighted the ecological implications of adding reactive nitrogen (N<sub>r</sub>) to terrestrial ecosystems. Seabird colonies represent a situation with concentrated sources of N<sub>r</sub>, through excreted and accumulated guano, often occurring in otherwise nutrient-poor areas. To date, there has been little attention given to modelling N flows in this context, and particularly to quantifying the relationship between ammonia (NH<sub>3</sub>) emissions and meteorology. This paper presents a dynamic mass-flow model (GUANO) that simulates temporal variations in NH<sub>3</sub> emissions from seabird guano. While the focus is on NH<sub>3</sub> emissions, the model necessarily also treats the interaction with wash-off as far as this affects NH<sub>3</sub>. The model is validated using NH<sub>3</sub> emissions measurements from seabird colonies across a range of climates, from sub-polar to tropical. In simulations for hourly time-resolved data, the model is able to capture the observed dependence of NH<sub>3</sub> emission on environmental variables. With temperature and wind speed having the greatest effects on emission for the cases considered. In comparison with empirical data, the percentage of excreted nitrogen that volatilizes as NH<sub>3</sub> is found to range from 2% to 67% (based on measurements), with the GUANO model providing a range of 2%–82%. The model provides a tool that can be used to investigate the meteorological dependence of NH<sub>3</sub> emissions from seabird guano and provides a starting point to refine models of NH<sub>3</sub> emissions from other sources.

© 2017 The Authors. Published by Elsevier Ltd. This is an open access article under the CC BY license (<http://creativecommons.org/licenses/by/4.0/>).

## 1. Introduction

Reactive nitrogen (N<sub>r</sub>) has been used to improve crop growth for

the last 8000 years (Bogaard et al., 2013). However, N<sub>r</sub> used as either manure or synthetic fertilizer has increased globally from approximately 21 Tg N yr<sup>-1</sup> in 1850 to 185 Tg N yr<sup>-1</sup> in 2000 (Potter et al., 2010). The consequences of applying N<sub>r</sub> to a surface depend on the climatic conditions, the properties of the substrate and the surrounding vegetation. Reactive nitrogen can either run off during rain events, become part of the surrounding ecosystem

\* Corresponding author. Centre for Ecology & Hydrology Edinburgh, Bush Estate, Penicuik, Midlothian, EH26 0QB, UK.

E-mail address: [sriddick@princeton.edu](mailto:sriddick@princeton.edu) (S.N. Riddick).

(immobilized in the soil or absorbed by plants) or volatilize as nitrogen-based gas: ammonia ( $\text{NH}_3$ ), nitrous oxide ( $\text{N}_2\text{O}$ ), nitrogen oxides ( $\text{NO}_x$ ) or nitrogen ( $\text{N}_2$ ). The rate of formation and volatilization of  $\text{NH}_3$  from  $\text{N}_r$  is highly temperature dependent (Sutton et al., 2013; Riddick et al., 2012, 2014) and  $\text{NH}_3$  emission has been linked with acidification and eutrophication close to the emissions site (Sutton et al., 2012) and changes in radiative forcing globally (Adams et al., 2001).

The largest seabird colonies are found in remote areas far from human interaction (Riddick et al., 2012). At such locations seabird nitrogen excreta is the dominant source of  $\text{N}_r$  making seabird colonies ideal “natural laboratories” to investigate biogeochemical processes and the resulting impact of  $\text{N}_r$  pathways on plants and animals. Studies have shown that seabirds are significant sources of  $\text{NH}_3$  (Wilson et al., 2004; Blackall et al., 2007; Zhu et al., 2011; Riddick et al., 2014, 2016) and have a large spatial impact in both the Arctic (Wentworth et al., 2015) and Antarctic (Theobald et al., 2013; Crittenden et al., 2015). Changes in atmospheric composition across the entire Baffin Bay region were attributed to seabird  $\text{NH}_3$  (Wentworth et al., 2015), while a study of Adelie penguin colony on the Antarctic continent suggested that volatilized  $\text{NH}_3$  creates a spatial impact zone of up to 300  $\text{km}^2$  surrounding the colony where phosphomonoesterase activity is increased in lichen populations (Crittenden et al., 2015).

Given the local and global importance of  $\text{NH}_3$  emissions, two main methods have been used to estimate  $\text{NH}_3$  emissions from  $\text{N}_r$  sources, which are broadly described as empirically derived emission factors and process-based models. The former use empirical data to integrate the effects of meteorology into a single value (‘emission factor’) that can be used, for example, to estimate emission of a particular animal species. Alternatively, the emission can be estimated based on a percentage of  $\text{N}_r$  that volatilizes as  $\text{NH}_3$ , e.g. on average 21% of N in manure volatilizes as  $\text{NH}_3$  in industrialized countries (Bouwman et al., 2002).

Process-based models attempt to replicate the effects of meteorology on the formation of  $\text{NH}_3$  from an  $\text{N}_r$  source.  $\text{NH}_3$  volatilization has been shown to increase at both high temperatures and high wind speeds (Demmers et al., 1998; Sommer and Christensen, 1991), while rain events may cause  $\text{NH}_3$  emissions to drop to almost zero, as illustrated by Sommer and Olesen (2000) for liquid manure spreading in Denmark. Most recent models calculate  $\text{NH}_3$  fluxes using Henry’s Law, i.e. the dissociation reactions of ammonium and  $\text{NH}_3$  in solution is used to calculate the  $\text{NH}_3$  gas on the surface, with the flux estimated using a resistance-based approach (e.g. Sutton et al., 1998; Cooter et al., 2010; Massad et al., 2010; Flechard et al., 2013). For instance, Cooter et al. (2010) used a process-based model to predict measured diurnal variation and daily means of  $\text{NH}_3$  emissions from agricultural soils.

Even though Henry’s Law has been used to calculate  $\text{NH}_3$  emissions from  $\text{N}_r$  sources, these models have not been explicitly validated with high resolution empirical measurements from a range of meteorological conditions. For example, Massad et al. (2010) reviewed existing measurements to compile a comprehensive dataset and derived generalized parameterizations for a range of fertilizers and ecosystems to be used in large-scale chemical transport and earth system models. Flechard et al. (2013) synthesized data from a range of studies to generate consistent parameterizations that can be used to calculate  $\text{NH}_3$  emissions on the regional and global scale. Cooter et al. (2010) used their model to calculate  $\text{NH}_3$  emissions at the field scale and compared their model output to fertilizer application at a site in North Carolina, USA.

In an initial approach to modelling  $\text{NH}_3$  emissions from seabirds, only the bioenergetics part of the GUANO model was used, linked to empirical estimates of the percentage volatilized (Wilson et al.,

2004; Blackall et al., 2007). This approach provided an adequate description of the spatial differences in  $\text{NH}_3$  emissions on a regional and country scale. However, it meant that there was a high uncertainty in the estimates in the extrapolations to a global scale by Blackall et al. (2007).

A first approach to address this uncertainty was provided by Riddick et al. (2012) who used an empirical temperature correction, with uncertainty ranges of estimates based on a) no temperature dependence and b) full solubility dependence according to the thermodynamics of Henry’s Law and ammonium dissociation. If, like Blackall et al. (2007), they ignored the possible effect of temperature, then they found total global  $\text{NH}_3$  emissions from seabirds of 442  $\text{Gg NH}_3 \text{ year}^{-1}$  (where penguins contributed 83%, due to improved bird statistics). By contrast, if  $\text{NH}_3$  emissions were proportional to the thermodynamic effect of temperature, they found total global  $\text{NH}_3$  emission from seabirds to be only 97  $\text{Gg NH}_3 \text{ year}^{-1}$  (where penguins contributed 63%). According to a mid-range estimate of the temperature dependence, they estimated 270  $\text{Gg NH}_3 \text{ year}^{-1}$  (with 80% from penguins). Penguins were thus estimated to be the main source of  $\text{NH}_3$  emissions from seabird colonies globally under all three scenarios, while this clearly shows the importance of addressing the temperature dependence of emissions.

The main limitation of Riddick et al. (2012) was the wide uncertainty range of their estimates and the need to constrain these by measurements, ideally using a process-based approach. A first application of the GUANO model reported by Sutton et al. (2013) to different sites globally showed that the main measured differences in the percentage of excreted guano that volatilizes as  $\text{NH}_3$  in relation to temperature could be reproduced.

This paper describes the GUANO model (Generation of emissions from Uric Acid Nitrogen Outputs), a dynamic mass-flow process-based model developed to simulate  $\text{NH}_3$  losses from seabird colonies. The model incorporates the main environmental factors affecting the volatilization process, allowing calculation of  $\text{NH}_3$  emissions from seabird-derived  $\text{N}_r$  on an hourly basis and upscaling to consider the effects of different meteorological conditions. The  $\text{NH}_3$  emissions simulated by the model are compared with  $\text{NH}_3$  emission estimates based on concentration measurements and turbulent exchange parameters from a climatically diverse set of seabird colonies. We use this comparison to investigate how  $\text{NH}_3$  emissions from seabirds vary with changing environmental conditions.

## 2. Methods and materials

### 2.1. Outline of the GUANO model

The GUANO model is designed to predict temporal variations in the formation of  $\text{NH}_3$  from a source of seabird-derived uric acid (Fig. 1). The model calculates  $\text{NH}_3$  emissions from a seabird colony using environmental variables and colony-specific data as input. Temperature, relative humidity, precipitation and wind speed are considered to have the greatest effect on  $\text{NH}_3$  formation and emission (Groot Koerkamp, 1994; Cooter et al., 2010; Massad et al., 2010; Flechard et al., 2013). The main elements of the model are described here, with additional details given in Supplementary Material Section 1.

The pathways taken by nitrogen following excretion as uric acid can be summarised in four steps (Fig. 1). Excreted guano forms uric acid (UA) that decomposes to form total ammoniacal nitrogen (TAN), which then partitions to form gaseous  $\text{NH}_3$ . Other pathways include wash-off of guano, UA and TAN from the surface at any stage during rain events. It should be noted that the loss of nitrogen due to plant uptake and immobilization, and other gaseous

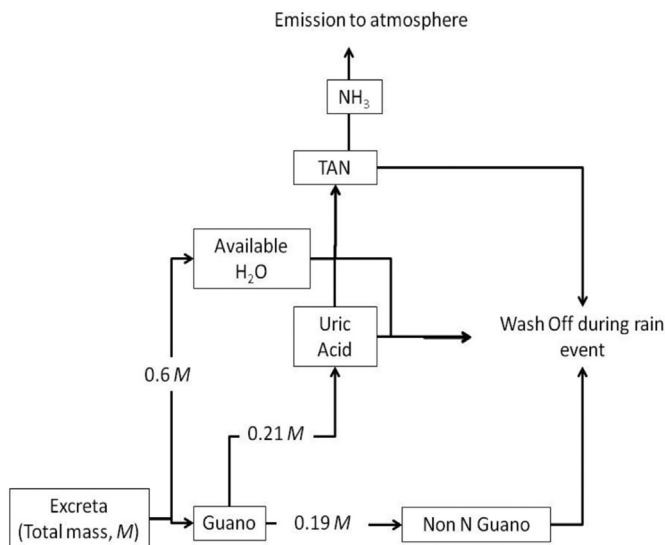


**Fig. 1.** Schematic of the GUANO model. Pathways taken by nitrogen following excretion as uric acid (after Blackall, 2004 modified). The numbers illustrate an example where the total mass of excreta ( $M$ ) is made from 0.6  $M$  of water, 0.21  $M$  of uric acid and 0.19  $M$  of non-N guano. TAN is Total Ammoniacal Nitrogen.

emissions, have not been included in the model since these are considered to take place on a slower time scale than  $\text{NH}_3$  emissions. The following steps are included in the model:

1. Nitrogen-rich guano, in the form of UA, is excreted onto the surface by seabirds at the colony. The amount of guano varies depending on the mass and behaviour of the nesting species (e.g. Wilson et al., 2004). At each time-step ( $t_N$ ), the UA budget ( $Q_{UA}$ ,  $\text{g m}^{-2}$ ) is calculated from the total nitrogen excreted ( $F_e$ ,  $\text{g m}^{-2} \text{hour}^{-1}$ ), the TAN produced per hour ( $F_{TAN}$ ,  $\text{g m}^{-2} \text{hour}^{-1}$ ) and the Uric acid nitrogen washed off by the rain ( $F_{w(UA)}$ ,  $\text{g m}^{-2} \text{hour}^{-1}$ ), where  $N$  is the hour of the year (Equation (1)).

$$Q_{UA}(t_{N+1}) = Q_{UA}(t_N) + F_e - F_{TAN} - F_{w(UA)} \quad (1)$$

2. Uric acid is converted to TAN, with the conversion rate depending on climatic conditions and the pH of the surface (Elliott and Collins, 1982; Elzing and Monteny, 1997; Groot Koerkamp et al., 1998). At each time step the TAN budget ( $Q_{TAN}$ ,  $\text{g m}^{-2}$ ) is calculated from the TAN produced per hour from UA ( $F_{TAN}$ ,  $\text{g m}^{-2} \text{hour}^{-1}$ ), the amount of  $\text{NH}_3$  emitted ( $F_{NH3}$ ,  $\text{g m}^{-2} \text{hour}^{-1}$ ) and the TAN washed off by the rain ( $F_{w(TAN)}$ ,  $\text{g m}^{-2} \text{hour}^{-1}$ ), where  $N$  is the hour of the year (Equation (2)).

$$Q_{TAN}(t_{N+1}) = Q_{TAN}(t_N) + F_{TAN} - F_{NH3} - F_{w(TAN)} \quad (2)$$

3. TAN partitions between  $\text{NH}_4^+$  and  $\text{NH}_3$  on the surface, with the position of the equilibrium depending on the pH and the temperature ( $T$ , K) of the surface (Equation (3)). A function,  $\Gamma = [\text{NH}_4^+]/[\text{H}^+]$ , is used to describe the equilibrium at the surface (Nemitz et al., 2000) such that the gaseous concentration of  $\text{NH}_3$  at the surface ( $X_c$ ) is:

$$X_c = \frac{161500}{T} \exp\left(\frac{-10378}{T}\right) \Gamma \quad (3)$$

The TAN concentration is a function of the water content of the guano. The water budget ( $Q_{H_2O}$ ,  $\text{kg m}^{-2}$ ) is calculated (Equation (4))

from the flux of water contained in excreted guano ( $F_{H_2O}(g)(g)$ ,  $\text{kg m}^{-2} \text{hr}^{-1}$ ), rain events ( $F_{H_2O}(pptn)$ ,  $\text{kg m}^{-2} \text{hr}^{-1}$ ), water run-off ( $F_{H_2O}(ro)$ ,  $\text{kg m}^{-2} \text{hr}^{-1}$ ) and evaporation ( $F_{H_2O}(evap)$ ,  $\text{kg m}^{-2} \text{hr}^{-1}$ ). Each of the parameters in Equation (4) is further described in the Supplementary Material Section 1.

$$Q_{H_2O}(t_{N+1}) = Q_{H_2O}(t_N) + F_{H_2O}(g) + F_{H_2O}(pptn) - F_{H_2O}(ro) - F_{H_2O}(evap) \quad (4)$$

4.  $\text{NH}_3$  on the surface volatilizes to the atmosphere, with the rate of volatilization (Equation (5)) depending on the  $\text{NH}_3$  concentration difference between the surface ( $X_c$ ) and the atmosphere ( $X_a$ ), the aerodynamic and boundary layer resistances ( $R_a$  and  $R_b$ ) (Sutton et al., 1993; Nemitz et al., 2001) estimating the effect of  $\text{NH}_3$  reabsorption by the substrate and any overlying vegetation using an empirical habitat factor ( $F_{hab}$ ). A habitat factor was used here in preference to a more process based description involving the bi-directional exchange of  $\text{NH}_3$  from vegetation because of the complexity of the mix of nesting types. The values of the habitat factors used are described in Section 2.2.3.

$$\text{NH}_3 \text{ emission} = \frac{X_c - X_a}{R_a + R_b} F_{hab} \quad (5)$$

## 2.2. Model input data

Site-specific  $\text{NH}_3$  emissions were calculated for five seabird colonies in a range climate zones: Tropical: Michaelmas Cay on the Great Barrier Reef (16.60 °S, 145.97 °E) and Ascension Island in the South Atlantic (7.99 °S, 14.39 °W), Temperate: the Isle of May in Scotland (56.19 °N, 2.56 °W) and Sub-Polar: Signy Island in the South Orkney Islands (60.72 °S, 45.60 °W) and Bird Island in South Georgia (54.0° S, 38.05° W).

### 2.2.1. Meteorological input data

To run the GUANO model, meteorological data are required for periods before, during and after the measurement campaigns. Continuous monitoring of the weather was conducted *in-situ* only on the Isle of May. For the other colonies, meteorological data (wind speed, ground temperature, relative humidity and rainfall) were collected during short term campaigns, with data beyond these periods obtained from the nearest meteorological station (Table 1).

### 2.2.2. Seabird colony data

The site-specific seabird data that have the greatest effect on the  $\text{NH}_3$  emission, as identified by Wilson et al. (2004), were collated from field observations and the literature: nest density and duration of the breeding season, adult mass, proportion of time spent at the colony (see Table 1 also Riddick et al., 2012). The estimated total nitrogen excreted at a colony is based on the assumption that adult seabirds excrete N at a constant rate while at the colony and away from it.

### 2.2.3. Habitat factors

Habitat factors ( $F_{hab}$ ) are used in Equation (5) to account for  $\text{NH}_3$  immobilized by the nesting substrate or recaptured by the overlying canopy and are listed in Table 1.1 in the Supplementary Material Section 1. This reflects a base value for bare rock of 1, where no  $\text{NH}_3$  is immobilized or recaptured, which is then reduced as a correction factor, to parameterise the effect of nesting behaviour of the birds. Following Wilson et al. (2004) and the

**Table 1**

Data used in the GUANO model.  $D_{met}$  is the distance from meteorological stations to each colony.  $F_{hab}$  values describe the fraction  $\text{NH}_3$  that is captured by the substrate and overlying vegetation (Supplementary Material Section 1, Table SM1.1). Site-specific seabird data input to the GUANO model were collated from field observation (nest density and duration of breeding season ( $D$ )) and from the literature (adult mass, fraction of time at colony ( $FC$ ), see Riddick et al., 2012). The nitrogen excretion rate at colony ( $F_e$ ) is calculated using Equation (1) in this study.

Colony	Target Species	Population (Pairs)	Measurement strategy	Av T (°C)	Av RH (%)	Av WS (m s <sup>-1</sup> )	$D_{met}$ (km)	$F_{hab}$	Adult Mass (g)	Nest Density (m <sup>-2</sup> )	Breeding season D (days)	FC	N excretion rate $F_e$ (g m <sup>-2</sup> hr <sup>-1</sup> )	Average Measured $\text{NH}_3$ Emission ( $\mu\text{g m}^{-2} \text{s}^{-1}$ )
Ascension Island 7.99 °S, 14.39 °W	Sooty tern	100,000	Active	27	72	5	2	0.67	190	1.26	122	0.6	0.14	30.2 <sup>a</sup>
Isle of May 56.19 °N, 2.56 °W	Atlantic puffin	20,000	Active	15	80	4	1	0.60	410	1.27	152	0.3	0.13	5.0 <sup>b</sup>
Bird Island 54.01 °S, 38.08 °W	Macaroni penguin	40,000	Active	3	92	5	5	1.00	4 680	0.85	213	0.6	1.13	12.9 <sup>b</sup>
Michaelmas Cay 16.60°S, 145.97°E	Common noddy	12,000	Passive	28	85	5	17	0.67	200	1.70	122	0.6	0.20	22.3 <sup>a</sup>
Signy Island 60.73° S, 45.58° W	Adélie and Chinstrap penguin	19,000	Passive	2	84	5	50	1.00	4 150	0.63	274	0.6	0.79	9.0 <sup>b</sup>

<sup>a</sup> Riddick et al. (2014).

<sup>b</sup> Riddick et al. (2016).

measurements of Riddick et al. (2012), habitat factors for birds that build nests on bare rock is taken as 1, while for those that nest on sand is taken as 0.67. For those bird species that nest on vegetation or use a nest,  $F_{hab}$  is 0.20 and birds excreting in burrows have a  $F_{hab}$  value of 0.

Penguins on Bird Island and Signy Island nest on bare rock ( $F_{hab} = 1$ ), while the birds on Michaelmas Cay and Ascension Island nest on sand ( $F_{hab} = 0.67$ ). On the Isle of May, adult puffins make burrows, but excrete outside, while their young excrete in burrows. Where adult puffins excrete depends on the time of day and climatic conditions: at dawn and dusk, large numbers of puffins can be seen on exposed rocks across the colony, and this also happens when it is warm and sunny. For the remainder of the time, puffins excrete on the soil outside their burrow. To accommodate variations in this assumption, the  $F_{hab}$  value for adult puffins was changed from vegetation only (0.2 as estimated by Wilson et al., 2004) to an  $F_{hab}$  value between rock and vegetation of 0.60 (average of 1 and 0.20). For puffin chicks, data suggest that these only excrete inside the burrows and leave the colony as soon as they leave the nest (Harris and Wanless, 2011). Puffin chicks are therefore not thought to contribute to seabird  $\text{NH}_3$  emission at the colony, with any emissions inside the burrows being absorbed by the soil inside the burrow, therefore  $F_{hab}$  for chicks is here set at 0.

#### 2.2.4. Other model inputs and implementation

Constant values are used in the model to describe the surface roughness length ( $z_0$ ) and the boundary layer Stanton number ( $B$ ) to calculate the turbulent atmospheric resistance ( $R_a$ ) and the quasi-laminar boundary layer resistance ( $R_b$ ) (Supplementary Material Section 1, equations SM21 and SM25). Constant values of 0.1 m and 5 were used in the model, and also varied as part of the model sensitivity analysis (Section 2.5). Based on reference Elliott and Collins (1982), the base-rate (at pH 9 and 35 °C) for the fraction of UA converted to TAN was 0.83% day<sup>-1</sup> (Supplementary Material Section 1). The pH of the guano within the model was set at 8.5, this value was based on measurements of Blackall (2004). Factors for wash-off under rain were assumed to be 1 and 0.5% mm<sup>-1</sup> rain for nitrogen and non-nitrogen, respectively (See Supplementary Material Section 1). Finally, based on data for remote marine environments (e.g., Sutton et al., 2003), background  $\text{NH}_3$  concentration was assumed to be 0.1  $\mu\text{g m}^{-3}$ .

The GUANO model was coded in Microsoft Excel. For each seabird colony the GUANO model uses meteorological and bird data to calculate the hourly  $\text{NH}_3$  emission ( $\text{g NH}_3 \text{ m}^{-2} \text{ h}^{-1}$ ). The annual  $\text{NH}_3$  emission is calculated as the sum of hourly emissions. The model runs were initialized with zero UA, TAN and water in the budgets starting at least 24 months before the assessment period for comparison with the emission estimates based on concentration measurements and turbulent exchange parameters.

#### 2.3. Model validation

The model setup and parametrization was set based on theoretical considerations and on available data to parametrize the model. In principle, the model set up was independent of measured validation data, according to the parameters considered. In the case of substrate pH and roughness length runs were based on a constant value, while TAN and Guano run off were based on a fixed percentage per mm of rain. The habitat factors were based on prior studies drawing on Blackall (2004), Wilson et al. (2004) and Blackall et al. (2007). The only parameter which was tuned according to measurements was  $F_{hab}$  at the Atlantic Puffin site on the Isle of May, Scotland. By contrast, the model tests in comparison with measurements at Mars Bay, Ascension Island, at Bird Island, South Atlantic, at Michaelmas Cay, Great Barrier Reef, at Signy Island, South Atlantic were made without tuning any other model parameters and therefore represent fully independent tests of the model in a wide range of climatic conditions.

##### 2.3.1. Measured $\text{NH}_3$ emissions for comparison with the model

Two methods were employed to conduct  $\text{NH}_3$  concentration emission estimates based on concentration measurements and turbulent exchange parameters, which were used to quantify  $\text{NH}_3$  emissions, as reported in detail by Riddick et al. (2014): (1) passive sampling and (2) active on-line  $\text{NH}_3$  analysis instrument. For the passive sampler measurements (ALPHA samplers, CEH Edinburgh, Tang et al., 2001), triplicate samplers were used at each sampling location and exposed for periods of 2–4 weeks to measure an average concentration for the exposure period. The time-averaged  $\text{NH}_3$  concentration data were then used with the WindTrax inverse dispersion model version 2.0 to calculate the emission (Flesch et al., 1995; Riddick et al., 2014).

Active on-line  $\text{NH}_3$  concentration measurements were made by Riddick et al. (2014, 2016) with an AiRRmonia gas analyser (Mechatronics, NL) on Bird Island and Ascension Island and a Nitrolux 1 000 gas analyser (Pranalytica, USA) on the Isle of May. The  $\text{NH}_3$  concentration data were averaged to 15-min data and used as input to the WindTrax in an inverse model to calculate the emission. The calculation of the  $\text{NH}_3$  emissions used as validation at each of the sites are the result of five separate field campaigns and are described in full in Riddick et al. (2014) for Michaelmas Cay and Ascension Island and Riddick et al. (2016) for Signy Island, the Isle of May and Bird Island (locations of the five fieldwork sites are presented in Supplementary Material Section 2).

As a result of the method employed at Michaelmas Cay and Signy Island (passive sampling only), hourly resolved measured  $\text{NH}_3$  fluxes were not available at these sites (Riddick et al., 2014, 2016). However, at Ascension Island (Riddick et al., 2014) and the Isle of May (Riddick et al., 2016), both passive (time integrated) measurements and the continuous measurements, were made allowing comparison between the two approaches. In both cases, close agreement was found between the passive (time-integrated) and active (time resolved) sampling methods, the uncertainty in chemical sampling method was  $\pm 20\%$  and  $\pm 12\%$  of the mean flux at the Isle of May and Ascension, respectively (Riddick et al. (2016). Calculation of a third estimate in each case (time-integrated based on the semi-continuous active sampling data) allowed it to be shown that the meteorological uncertainties associated with long measurement periods (for the passive, time-integrated measurements) were of similar magnitude to the uncertainties between the two different chemical sampling methods.

#### 2.4. Comparison modelled emissions to those estimated through measurement

The GUANO model simulations were validated with emission estimates based on concentration measurements and turbulent exchange parameters from the five field sites. To assess the fit of the model, the hourly measured emissions were plotted against the hourly modelled  $\text{NH}_3$  emissions, with the slope, intercept and determination coefficient ( $R^2$ ) of the linear regression calculated. Time-averaged modelled emissions are also presented and compared against matched time-averaged emission estimates based on concentration measurements and turbulent exchange parameters to show that the model, not only captures the hourly emissions, but also is consistent with measurements over a period of time.

In addition, the mean  $\text{NH}_3$  emission for each colony was calculated (in  $\mu\text{g m}^{-2} \text{s}^{-1}$ ) from the hourly emissions. The percentage of nitrogen volatilized ( $P_v$ ) was calculated from the total nitrogen excreted at each colony during the measurement period and the total nitrogen estimated to be volatilized as  $\text{NH}_3$  over the same period.

#### 2.5. $\text{NH}_3$ emission and meteorology

To investigate the effects of meteorology, the slope, intercept and  $R^2$  between modelled  $\text{NH}_3$  emission and each variable was calculated. The coefficient of determination is used to assess the size of the effect each environmental variable (ground temperature, wind speed, relative humidity and precipitation) has on the modelled  $\text{NH}_3$  emission so that the key drivers of emission at each measurement site can be identified.

#### 2.6. Sensitivity analysis

A sensitivity study was performed on the GUANO model to

determine the most significant model parameters in relation to the model output. The following model parameters were investigated with realistic variations in each input parameter:  $z_0$  (m), fraction of UA converted to TAN per day, percentage nitrogen wash off (%  $\text{mm}^{-1}$  rain), percentage non-nitrogen wash-off (%  $\text{mm}^{-1}$  rain), pH, habitat factors ( $F_{hab}$ ), boundary layer Stanton number ( $B$ ), temperature ( $T$ ,  $^{\circ}\text{C}$ ), relative humidity ( $RH$ , %), wind speed ( $U$ ,  $\text{m s}^{-1}$ ), precipitation ( $P$ ,  $\text{mm m}^{-2} \text{hr}^{-1}$ ), net solar radiation ( $Rn$ ,  $\text{W m}^{-2}$ ), pH and background  $\text{NH}_3$  concentration ( $\mu\text{g m}^{-3}$ ). The sensitivity of the  $\text{NH}_3$  emissions to each input parameter was tested using the GUANO model application to the Atlantic puffin colony on the Isle of May. The application of the GUANO model at Isle of May was used in the sensitivity analysis because this temperate site could best respond to positive and negative changes in environmental conditions in a global context.

### 3. Results

#### 3.1. Model output and validation with empirical data

##### 3.1.1. Mars Bay, Ascension Island: sooty tern colony

The  $\text{NH}_3$  emissions calculated by the GUANO model for Ascension Island show a strong diurnal pattern, with the peak emissions corresponding to the hottest, most turbulent and windiest part of the day. The maximum measured emission during the study period was  $370 \mu\text{g NH}_3 \text{ m}^{-2} \text{ s}^{-1}$  (Fig. 2). The  $\text{NH}_3$  emissions calculated by the GUANO model for Ascension Island are in close agreement to those derived from field measurements (Table 3; Supplementary Material Section 2 Fig. SM 2.1), with a linear regression slope of 1.07, intercept of  $-1.20 \mu\text{g m}^{-2} \text{ s}^{-1}$  and  $R^2 = 0.94$ . The average modelled  $\text{NH}_3$  emission for Ascension Island during the measurement period was  $22.3 \mu\text{g NH}_3 \text{ m}^{-2} \text{ s}^{-1}$ , the average measured  $\text{NH}_3$  emission on Ascension was  $22.3 \mu\text{g NH}_3 \text{ m}^{-2} \text{ s}^{-1}$  and the average modelled  $\text{NH}_3$  emission for periods when measurement data available was  $19.8 \mu\text{g NH}_3 \text{ m}^{-2} \text{ s}^{-1}$ . The most notable features of the modelled and measured  $\text{NH}_3$  emission is the strong dependence on temperature and moisture availability (with higher emissions after rain events on 25 May and 6–7 June), with the TAN budget almost fully depleted before then end of each day. This implies that the  $\text{NH}_3$  emission rate is tightly coupled to the TAN production rate at this site (Supplementary Material Section 3 Fig. SM 3.1; Supplementary Material Section 4 Fig. SM 4.1,  $R^2$  value = 0.98). At this site, aerodynamic and boundary layer resistance has little effect, as the TAN produced is all quickly lost through  $\text{NH}_3$  emissions. Ammonia emission is thus hydrolysis-limited for the test period at this site, with the performance of the GUANO model therefore depending almost entirely on its parametrization of the urea hydrolysis rate.

##### 3.1.2. Isle of May, Scotland: Atlantic puffin colony

The modelled emissions were lower for the Isle of May puffin colony than Ascension Island (Sooty tern), but showed a similar diurnal pattern (Fig. 3), with high emissions in the day (maximum of  $25 \mu\text{g m}^{-2} \text{ s}^{-1}$  during the afternoon) and negligible emissions at night. When compared with the emission estimates based on concentration measurements and turbulent exchange parameters, the hourly  $\text{NH}_3$  emissions modelled by the GUANO model were underestimated, with a linear regression slope of 0.13, intercept of  $5.7 \mu\text{g m}^{-2} \text{ s}^{-1}$  and  $R^2$  of 0.13 (Table 3; Supplementary Material Section 2 Fig. SM 2.2). The poorest fit occurred on 1st July 2009, where the model overestimated the measured  $\text{NH}_3$  emission during the early hours of the morning. This was associated with a period of low-wind speed and stable conditions, which could also reflect uncertainties in the measurement estimate at this time. During the period of 29 June to 2 July the measured emissions were

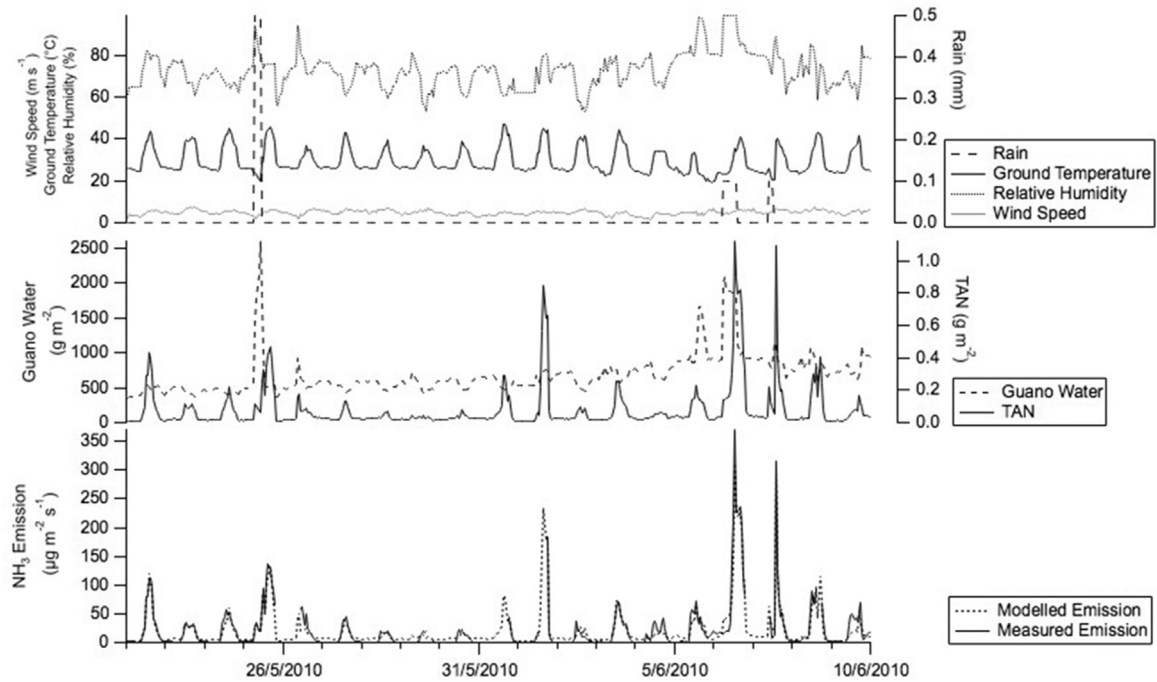


**Fig. 2.** Comparison between measured and modelled  $\text{NH}_3$  emissions for the Sooty tern colony at Mars Bay, Ascension Island (22nd May to 10th June 2010). Top panel: Rain, ground temperature, relative humidity and wind speed (measured values). Middle panel: Guano water and TAN (modelled values). Bottom Panel: Measured and modelled  $\text{NH}_3$  emissions. The  $F_{hab}$  value used in the GUANO model was 0.67 (based on a sand substrate). All values are hourly; tick marks on the x-axis indicate midnight.

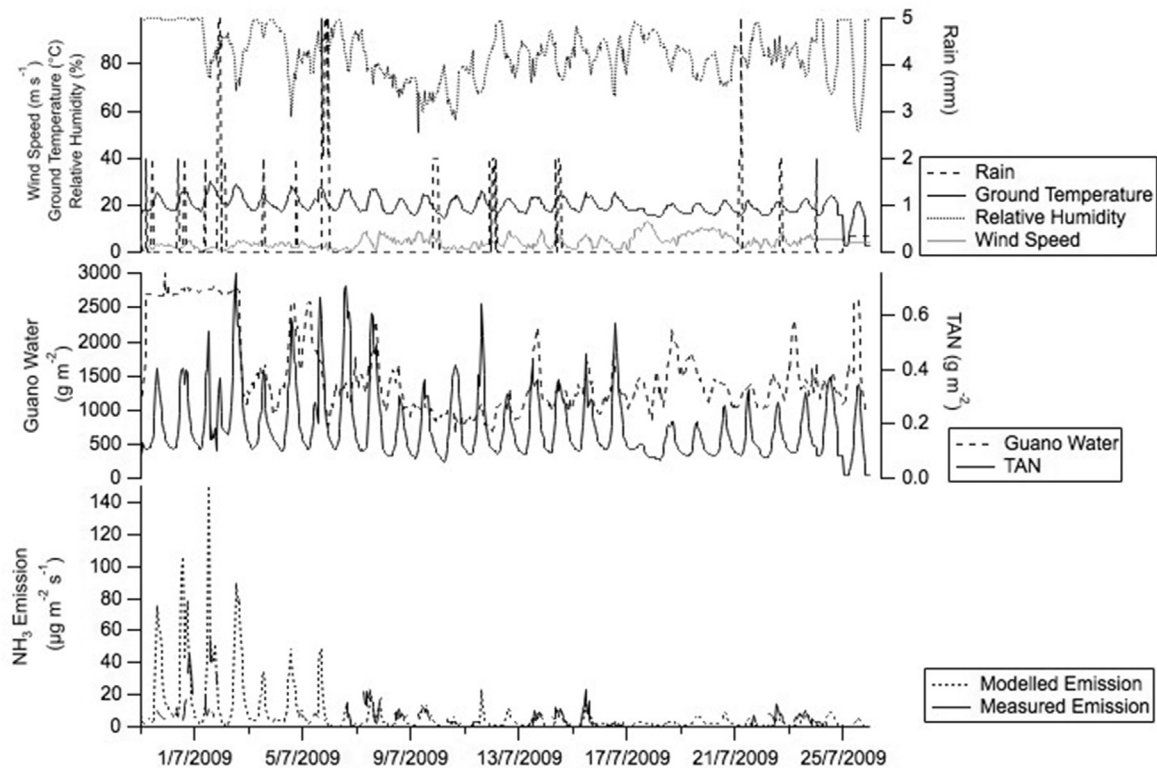


**Fig. 3.** Comparison between measured and modelled  $\text{NH}_3$  emissions for the Isle of May, Scotland (5th to 26th July 2009). Top panel: Rain, ground temperature, relative humidity and wind speed (measured values). Middle panel: Guano water and TAN (modelled values). Bottom Panel: Measured and modelled  $\text{NH}_3$  emission. The  $F_{hab}$  value used in the GUANO model was 0.64 (based on a soil/rock substrate). All values are hourly; tick marks on the x-axis indicate midnight.

much smaller than model and this may correspond to a period of foggy weather where  $\text{NH}_3$  could have dissolved in the fog and few puffins were seen around the colony, which may explain why the measured emissions were much smaller than the modelled emissions, which did not take account of this meteorological interaction with the ammonia gas, local bird behaviour and movements.

The average modelled  $\text{NH}_3$  emission for the Isle of May during the measurement period was  $7.7 \mu\text{g NH}_3 \text{ m}^{-2} \text{ s}^{-1}$ , the average measured  $\text{NH}_3$  emission on the Isle of May was  $6.9 \mu\text{g NH}_3 \text{ m}^{-2} \text{ s}^{-1}$  and the average modelled  $\text{NH}_3$  emission for periods when measurement data available was  $9.3 \mu\text{g NH}_3 \text{ m}^{-2} \text{ s}^{-1}$ . At this site the TAN budget fluctuates greatly, with hourly modelled and measured emissions correlated with the TAN budget (Supplementary Material Section 3 Fig. SM 3.2,  $R^2 = 0.05$ ). In contrast to Ascension Island, however, TAN did not deplete to near zero each evening, indicating that daily  $\text{NH}_3$  emission is only partially limited by TAN production over the previous 24 h.

### 3.1.3. Bird Island, South Atlantic: macaroni penguin colony 'Big Mac'

Compared with the other seabird colonies considered in this study, a diurnal pattern was much less noticeable for both modelled and measured  $\text{NH}_3$  emissions from the Macaroni penguin colony on Bird Island (Fig. 4). The maximum  $\text{NH}_3$  emission simulated by the GUANO model from the colony was  $53 \mu\text{g NH}_3 \text{ m}^{-2} \text{ s}^{-1}$  at 0500 on 11th December 2010. Contrary to the other sites, there was also little correlation between the emission rate and ground temperature, which was associated with small variation in ground temperature (3–8 °C range) during the measurement period. Instead, at this site the periods of lowest  $\text{NH}_3$  emissions (below  $10 \mu\text{g NH}_3 \text{ m}^{-2} \text{ s}^{-1}$ ) were observed during periods of lower wind speed, with maximum emissions during periods of high wind speed, linked to a substantial range of wind speed during the measurement period (0.3–12  $\text{m s}^{-1}$ ). The GUANO model simulations reproduced the measured  $\text{NH}_3$  emissions well, with a linear regression slope of

1.09, and intercept of  $-1.32 \mu\text{g m}^{-2} \text{ s}^{-1}$  and  $R^2 = 0.86$  (Table 3; Supplementary Material Section 2 Fig. SM 2.3). Modelled emissions from the Big Mac colony are mostly between 0 and  $20 \mu\text{g m}^{-2} \text{ s}^{-1}$ . The average modelled  $\text{NH}_3$  emission for Bird Island during the measurement period is  $13.4 \mu\text{g NH}_3 \text{ m}^{-2} \text{ s}^{-1}$ , the average measured  $\text{NH}_3$  emission on Bird Island was  $12.3 \mu\text{g NH}_3 \text{ m}^{-2} \text{ s}^{-1}$  and the average modelled  $\text{NH}_3$  emission for periods when measurement data available was  $12.4 \mu\text{g NH}_3 \text{ m}^{-2} \text{ s}^{-1}$ .

At this site, the modelled TAN budget can be seen from Fig. 4 to show negligible fluctuation on a daily time scale, contrary to Ascension Island and the Isle of May (Supplementary Material Section 4), while showing a slight increase over the first period and first decrease then increase over the second period. At the same time this site has much larger amounts of available TAN at the surface than these other sites, at 2–3  $\text{g m}^{-2}$ . With relatively modest temperature fluctuations during the measurement period, at this site, the variation in  $\text{NH}_3$  emission rate can therefore be seen to be primarily limited by the mass transfer process itself, as affected by wind speed and surface temperature. Supplementary Material Section 3 Fig. SM 3.3 shows that there is still a significant correlation between simulated TAN production and  $\text{NH}_3$  emission ( $R^2 = 0.29$ ), the relationship is less than at the temperate and tropical sites.

The TAN production rate at Bird Island ( $0\text{--}0.15 \text{ g m}^{-2} \text{ hr}^{-1}$ ) is more similar to the Isle of May ( $0\text{--}0.4 \text{ g m}^{-2} \text{ hr}^{-1}$ ) than Ascension Island ( $0\text{--}0.1 \text{ g m}^{-2} \text{ hr}^{-1}$ ) (Supplementary Material Section 3 Figs. SM 3.1, SM 3.2 and SM 3.3). This suggests that, while temperature does not affect the daily variation, the overall magnitude of  $\text{NH}_3$  emission is still largely controlled by TAN hydrolysis rate, i.e. hydrolysis rate controls the overall rate of emission while meteorology controls the short-term variation in  $\text{NH}_3$  emission.

### 3.1.4. Michaelmas Cay, Great Barrier Reef: common noddy colony

The  $\text{NH}_3$  emissions simulated by the GUANO model for Michaelmas Cay show a strong diurnal pattern, with maximum

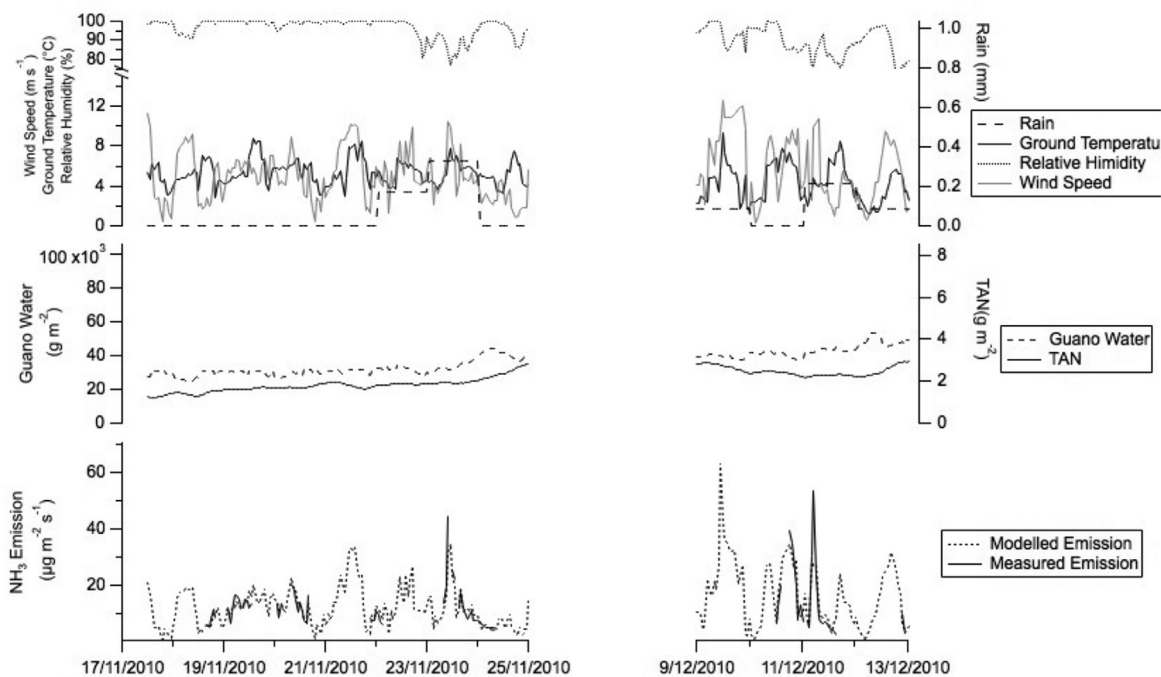


Fig. 4. Comparison of measured and modelled  $\text{NH}_3$  emissions from the Big Mac Macaroni penguin colony, Bird Island, South Georgia (18/11/2010 to 13/12/2010). Top panel: Rain, ground temperature, relative humidity and wind speed (measured values). Middle panel: Guano water and TAN (modelled values). Bottom panel: Measured and modelled  $\text{NH}_3$  emission. The  $F_{hab}$  value used in the GUANO model was 1 (based on a rock substrate). All values are hourly; tick marks on the x-axis indicate midnight.

emissions during the day reaching nearly  $500 \mu\text{g m}^{-2} \text{s}^{-1}$  which drop to an emission during the night of between 1 and  $10 \mu\text{g m}^{-2} \text{s}^{-1}$ . The average  $\text{NH}_3$  emission measured using passive samplers for two periods of four weeks during November and December (Riddick et al., 2014) are very similar to the emissions simulated by the GUANO model when averaged over the same periods (Fig. 5A and Table 2). The  $\text{NH}_3$  emissions measured during the field campaign are  $25.9 \mu\text{g NH}_3 \text{ m}^{-2} \text{ s}^{-1}$ . Both measured and modelled emission showed an increase from November to December. The average  $\text{NH}_3$  emission predicted by the GUANO model is  $27.5 \mu\text{g NH}_3 \text{ m}^{-2} \text{ s}^{-1}$  for November and December 2009.

The modelled TAN budget showed a high level of temporal structure, combining both substantial diurnal variations (indicating some limitation according to the TAN production rate) and some variation due to mass transfer limitations under the control of temperature and other environmental variables (see Supplementary Material Section 3 Fig. SM 3.4, where simulated TAN production rate and simulated  $\text{NH}_3$  emission are found to be correlated with  $R^2 = 0.91$ ).

### 3.1.5. Signy Island, South Atlantic: chinstrap penguin colony

As with the tropical and temperate regions, but in contrast to

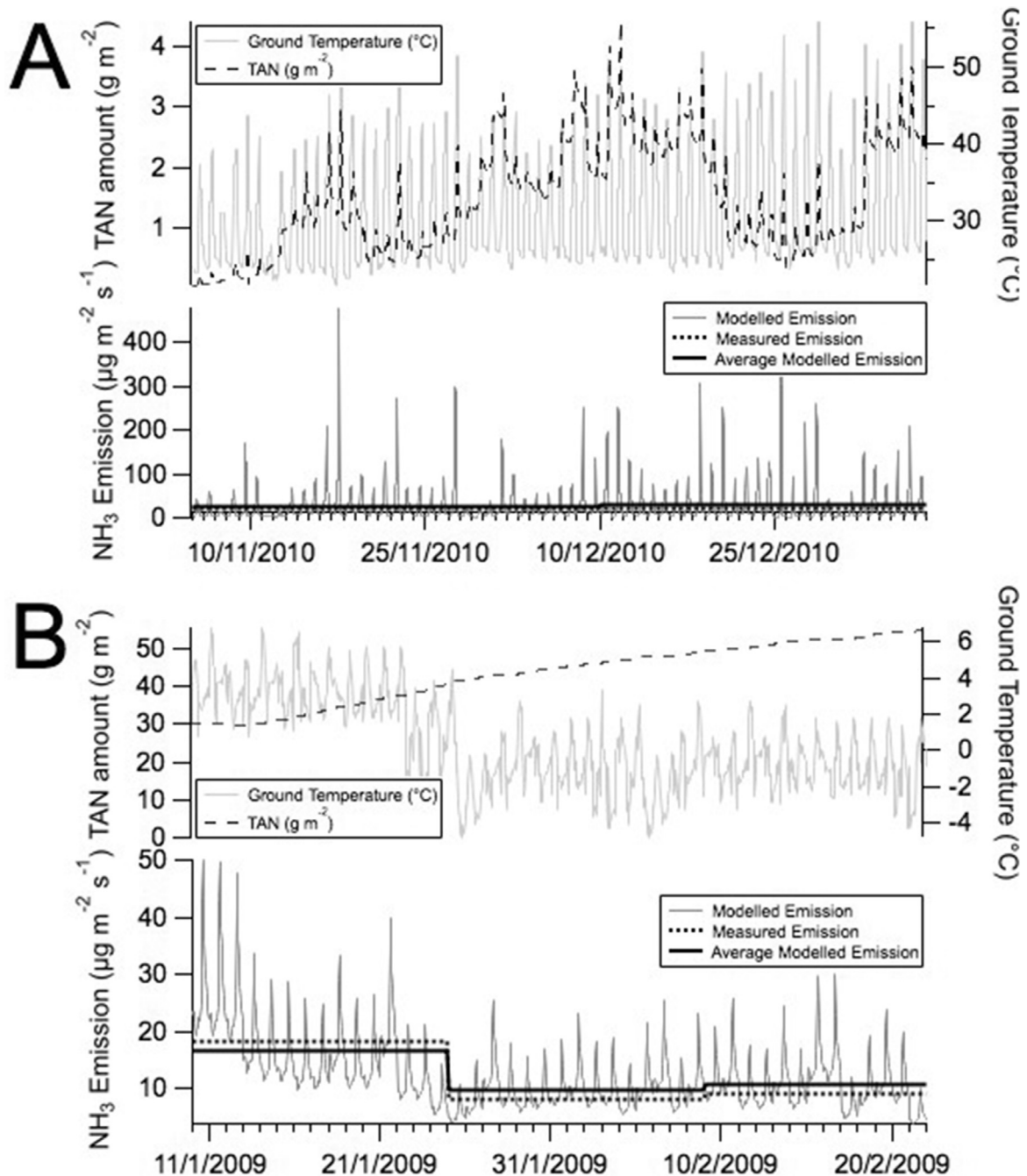


**Fig. 5.** Comparison between monthly time-integrated measured  $\text{NH}_3$  emission with modelled hourly  $\text{NH}_3$  emissions and monthly-mean modelled emissions for A. Michaelmas Cay, Great Barrier Reef, Australia (5/11/2009 to 1/1/2010) and B. Signy Island (10/01/09 to 21/02/09). Measured ground temperature (°C) and modelled TAN amount ( $\text{g m}^{-2}$ ) are shown for comparison. Tick marks on the x-axis indicate midnight. The  $F_{\text{hab}}$  values were 0.67 (sand) and 1 (rock) for Michaelmas Cay and Signy Island, respectively.

**Table 2**  
Comparison between the measured NH<sub>3</sub> emissions and NH<sub>3</sub> emissions simulated using the GUANO model for Michaelmas Cay, Great Barrier Reef, Australia during Period 1 (5/11/2009 to 10/12/2009) & Period 2 (10/12/2009 to 6/1/2010) and Signy Island during Period 1 (10/01/09–25/01/09), Period 2 (25/01/09–08/02/09) and Period 3 (08/02/09–21/02/09). Measured values from Riddick et al. (2014, 2016).

	Michaelmas Period 1	Michaelmas Period 2	Signy Period 1	Signy Period 2	Signy Period 3
Measured emission ( $\mu\text{g NH}_3 \text{ m}^{-2} \text{ s}^{-1}$ )	21.3	22.2	18.2	7.9	9.0
GUANO Model emission ( $\mu\text{g NH}_3 \text{ m}^{-2} \text{ s}^{-1}$ )	25.1	29.9	16.7	9.7	10.7
Difference between measured and modelled (%)	15.0	25.8	-8.3	22.9	18.4

the other sub-polar colony at Bird Island, NH<sub>3</sub> emissions simulated for Signy by the GUANO model were strongly diurnal (Fig. 5B). This can be explained by the more regular diurnal variation in temperature (typically 4–6 °C diurnal change) than at Bird Island (Fig. 4).

The Signy Island colony is used by both Adélie and Chinstrap penguins for the first measurement period. During the second period, the Adélie penguins gradually left the colony and only Chinstrap penguins were present for the third period. The NH<sub>3</sub> emissions at Signy Island are the highest for the first period, reaching a maximum of 50.0  $\mu\text{g NH}_3 \text{ m}^{-2} \text{ s}^{-1}$ . The average NH<sub>3</sub> emission predicted by the GUANO model for the penguin colony during the whole measurement period was 10.7  $\mu\text{g NH}_3 \text{ m}^{-2} \text{ s}^{-1}$ . This is similar to the NH<sub>3</sub> emissions measured during the field campaign of 9.0  $\mu\text{g NH}_3 \text{ m}^{-2} \text{ s}^{-1}$  (Table 2).

The simulated TAN budget for the penguin colony at Signy Island shows negligible diurnal variation, but rather a steady increase through the study period from 30 to 55  $\text{g m}^{-2}$  (Fig. 5). Overall, there was only a weak correlation between simulated TAN production and simulated NH<sub>3</sub> emission (Supplementary Material Section 3 Fig. SM 3.5). The reason for the smooth trend in TAN budget at the surface (Fig. 5b) is that the NH<sub>3</sub> emissions and run off during the study period represent only small fraction of the TAN produced (Supplementary Material Section 4 Figure SM 4.5). The values of the TAN budget at Signy Island are much higher than the other sites because of the lower temperatures that allow TAN to accumulate rather than volatilize.

### 3.2. NH<sub>3</sub> emissions and environmental conditions

Considering the simulated estimates from the GUANO model at each site, the strongest meteorological driver of NH<sub>3</sub> emission was

found to be ground temperature for all sites except for Bird Island, average  $R^2$  of 0.29 (range 0.11–0.39) (Table 3). As ground temperature increases, the rate of bacterial decomposition of uric acid nitrogen to form TAN (Equation (2)) increases and, coupled with an increased volatility of NH<sub>3</sub> (Equation (3)), results in increased NH<sub>3</sub> emission.

The next strongest driver of NH<sub>3</sub> emission is wind speed, with an average  $R^2$  of 0.18 (range 0.01–0.59), with the highest correlation on Bird Island ( $R^2 = 0.59$ ) where there was a wide range of wind speeds and small differences in temperature. Relative humidity and precipitation were not found to be strong climatic drivers of NH<sub>3</sub> emission, with  $R^2$  values ranging from 0.01 to 0.04. This is not to say that these factors are unimportant, as the response of both modelled and measured NH<sub>3</sub> emission to precipitation at Ascension Island showed (Fig. 2). Precipitation and relative humidity are fundamental controls on TAN formation from UA and influences NH<sub>3</sub> emission on a longer time scale than variation in temperature and wind speed which directly affects the hourly variation in NH<sub>3</sub> emissions.

The importance of moisture availability which is absorbed by guano may be more easily seen in the measured long-term response, where Michaelmas Cay had a higher measured percentage volatilization ( $P_v = 67\%$ ) as compared with Ascension Island ( $P_v = 52\%$ ) even though the sites had similar average temperature (Tables 1 and 3). This may be reflective of more moisture limitation to uric acid hydrolysis at Ascension Island. This difference is supported by the GUANO model simulation which also estimated a higher value of  $P_v$  for Michaelmas Cay (82%) than for Ascension Island (37%), reflecting the generally higher simulated guano water content at Michaelmas Cay than at Ascension Island (Figs. 5A and 2).

**Table 3**  
Comparison between measured NH<sub>3</sub> emissions and NH<sub>3</sub> emission simulated using the GUANO model for the measurement periods at different study sites.  $P_v$  is the percentage of N volatilized as NH<sub>3</sub>. Determination coefficients ( $R^2$ ) are shown for modelled emissions based on hourly data between modelled NH<sub>3</sub> emission and each climate variable and for the comparison of modelled and measured emissions (value after each  $R^2$  in brackets shows + or - interaction). The mean modelled % of available TAN emitted was calculated from the total emission and the total duration of the measurement period. The climate variables  $T_g$  represents Ground Temperature,  $RH$  is relative humidity,  $WS$  is wind speed and  $P$  is precipitation. For Michaelmas Cay and Signy Island, denoted by <sup>a</sup>, the values are a time-weighted mean of the measurement and model values shown in Table 2.

Colony	NH <sub>3</sub> emission ( $\mu\text{g m}^{-2} \text{ s}^{-1}$ )		$P_v$ (%)	$R^2$ between hourly modelled NH <sub>3</sub> emission and meteorological variable				Comparison of hourly modelled to hourly measured emissions			
	Measured	GUANO Model		$T_g$	$RH$	$WS$	$P$	$R^2$	Slope	Intercept ( $\mu\text{g m}^{-2} \text{ s}^{-1}$ )	Modelled mean % of available TAN emitted as NH <sub>3</sub> in a day <sup>A</sup>
Ascension Island	30.2	21.5	51.9	0.11	0.01	0.01	0.03	0.94	1.07	-1.2	67.0
Isle of May	5.0	3.2	4.7	0.39	0.04	0.06	0.01	0.13	0.13	5.7	5.5
Bird Island	12.9	12.7	1.8	0.39	0.04	0.59	0.01	0.86	1.09	-1.3	1.6
Michaelmas Cay <sup>a</sup>	22.3	27.5	66.8	0.18	0.04	0.01	0.01				20.9
Signy Island <sup>a</sup>	9.0	10.7	2.4	0.38	0.03	0.22	0.01				0.11

<sup>A</sup> This is defined as the average percentage of TAN produced in a day that volatilizes as NH<sub>3</sub>.

### 3.3. Sensitivity analysis

A sensitivity analysis of the GUANO model is shown in Table 4 for each input variable selected. The estimated NH<sub>3</sub> emissions were most sensitive to changes in environmental variables, with highest sensitivity to ground temperature which varied by +59.9% to –36.8% for changes of +10% and –10%, respectively. The NH<sub>3</sub> emissions calculated by the GUANO model had the smallest response to changes in micrometeorological constants used to calculate the flux, i.e. surface roughness, boundary layer Stanton number and background NH<sub>3</sub> concentration.

Of the constants used, the GUANO model is most sensitive the substrate pH. The model uses a substrate pH equal to the pH of guano, estimated at 8.5 (hydron concentration: [H<sup>+</sup>] = 3.2E-9) by Blackall (2004), and changes in pH from pH 7 ([H<sup>+</sup>] = 1E-7) to pH 10 ([H<sup>+</sup>] = 1E-10) result in 73% and –22% effect on NH<sub>3</sub> emission, respectively. The sensitivity in the model to pH is caused by the  $\Gamma$  function, which is used to describe the equilibrium of the concentrations of the TAN and hydrogen ions on the surface (Equation SM18), and is directly proportional to the gaseous concentration of NH<sub>3</sub> at the surface (Equation (3)). We recognize that this is a source of uncertainty in the model, however the value used in the GUANO model for substrate pH is currently the best available.

The sensitivity of the modelled emission to changing environmental conditions can be seen in Supplementary Material Section 6, where in all cases the NH<sub>3</sub> emission increases with ground temperature and in all cases emissions is the same at 25 °C. Wind speed has the next biggest effect as NH<sub>3</sub> emission increases with wind speed at low temperatures. Precipitation also affects emission as higher rainfall results in lower emission at low temperatures. Relative humidity has relatively little effect on emission, but higher humidity results in lower emission.

## 4. Discussion

### 4.1. General discussion

This paper presents and describes the GUANO model, the first dynamic mass-flow process-based model developed to simulate NH<sub>3</sub> losses from seabird guano, which is here validated against NH<sub>3</sub>

emissions measured at seabird colonies representative of a range of climates around the world. Comparison with NH<sub>3</sub> emission estimates based on measurements of NH<sub>3</sub> concentration and turbulent exchange parameters (Riddick et al., 2014, 2016) shows that the model is able to reproduce the magnitude and temporal variation of NH<sub>3</sub> emissions for a broad range of nesting habitats and climatic conditions. The GUANO model has been structured to simulate hourly NH<sub>3</sub> emission, using nitrogen excretion rates, temperature, relative humidity, wind speed and precipitation. This choice of time resolution, however, is purely a matter of model implementation and the model has the flexibility to allow for this to be changed. However, the advantage of calculating hourly emission estimates is that the GUANO model is able to discriminate the main effects of varying environmental conditions including diurnal variability. In this way, a clearer picture emerges of the main controls on NH<sub>3</sub> emissions from seabird colonies.

The model parametrization was based primarily on well-established existing principles and measured terms. Elements such as the turbulent and laminar boundary layer resistances have been widely used in other models, where the main uncertainty concerns the setting of the surface roughness length. Here we used an estimate based on observational data (Riddick et al., 2014, 2016) and Seinfeld and Pandis (2006) to set the roughness length at 0.1 m. The emission itself is driven by the concentration difference between atmospheric NH<sub>3</sub> concentrations and the surface NH<sub>3</sub> concentration. However, as the former is very small, the key uncertainty is the surface NH<sub>3</sub> concentration. The first challenge is to simulate the rate of uric acid hydrolysis, for which we used a parametrization unchanged from Elliott and Collins (1982), based on measurements from a poultry house context. The fact that this delivers good agreement with observed fluxes in a context where NH<sub>3</sub> emission is limited almost entirely by UA hydrolysis rate (Ascension Island), provides strong support for the parametrization of Elliott and Collins (1982). The other major uncertainties in the model concern surface pH, the habitat factor and the extent of wash-off. For the surface pH use of a prior measurement estimate from Blackall (2004) for all modelling sites shows that a fixed value of pH 8.5 is sufficient for the model application. The  $F_{hab}$  could be considered as a model tuning parameter, however, this would only apply for sites not on bare rock (for which  $F_{hab} = 1$ ). The reduction

**Table 4**

Sensitivity analysis of total modelled NH<sub>3</sub> emission for the Isle of May (28/06/10 to 23/07/10) using the GUANO model. C indicates a constant and V indicates a variable. For the meteorological variables, each hourly value used for ground temperature, relative humidity, wind speed, precipitation and net solar radiation is varied by  $\pm 10\%$ . + the average value for each meteorological variable from 28/06/10 to 23/07/10 is given. \* denotes  $F_{hab}$  for the Isle of May, other  $F_{hab}$  values are given in Table 1.1 in Supplementary Material Section 1.

Factor	Type	Base value for all model runs (and range tested)	Source of base value	% Change in NH <sub>3</sub> emission	
				High Value	Low Value
Surface roughness height ( $z_0$ , m)	C	0.1 (0.01–0.5)	Seinfeld and Pandis (2006) Riddick et al. (2014, 2016)	+70	–56
UA conversion to TAN (% day <sup>-1</sup> at pH 9, T = 35 °C)	C	0.83 ( $\pm 10\%$ )	Elliott and Collins (1982)	–9.42	9.30
Nitrogen wash off (% mm <sup>-1</sup> rain)	C	1 ( $\pm 10\%$ )	Blackall (2004)	8.19	–7.12
Non-Nitrogen Wash off (% mm <sup>-1</sup> rain)	C	0.5 ( $\pm 10\%$ )	Blackall (2004)	–0.15	+0.17
Boundary layer Stanton number ( $B$ )	C	5 ( $\pm 10\%$ )	Sutton et al. (1993)	+0.04	–0.04
Habitat Factor ( $F_{hab}$ ) <sup>*</sup>	C	0.60 (0.2–1)	Wilson et al. (2004) Riddick et al. (2012)	–70	+49
Substrate pH	C	8.5 (7–9)	Blackall (2004)	+73	–22
Background NH <sub>3</sub> concentration ( $\mu\text{g m}^{-3}$ )	C	0.1 ( $\pm 10\%$ )	Sutton et al. (2003)	–0.02	+0.01
Ground Temperature ( $T$ , °C)	V	20 <sup>+</sup> ( $\pm 10\%$ )	Measured	–36.8	+59.9
Relative Humidity ( $RH$ , %)	V	84 <sup>+</sup> ( $\pm 10\%$ )	Measured	–13.0	+6.7
Wind Speed ( $U$ , m s <sup>-1</sup> )	V	4.3 <sup>+</sup> ( $\pm 10\%$ )	Measured	–11.0	+12.9
Precipitation ( $P$ , mm m <sup>-2</sup> hr <sup>-1</sup> )	V	0.17 <sup>+</sup> ( $\pm 10\%$ )	Measured	+20.7	–11.8
Net solar radiation ( $R_n$ , Wm <sup>-2</sup> )	V	82.6 <sup>+</sup> ( $\pm 10\%$ )	Measured	–2.1	+1.2

factors used in this study were in fact based on prior estimates from Wilson et al. (2004) with the only changes for this study being at the Atlantic puffin site on the Isle of May where  $F_{hab}$  was taken as an average of rock and vegetation nesters to reflect the variability of the bird's behaviour. For the wash off factors, constant relationship for all sites was used of 1 and 0.5%  $\text{mm}^{-1}$  rain for nitrogen and non-nitrogen, respectively. While this is an extremely simple approach, its value was based on Blackall (2004) and thus set as a prior value rather than being used to fit the measurements. Overall, therefore, it can be seen that while the performance of the model runs is sensitive to the model parametrization, the parameter choices were largely based on prior estimates independently from the outcome of the measurements.

The comparison of the GUANO model output with  $\text{NH}_3$  emission estimates based on concentration measurements and turbulent exchange parameters at a range of sites showed the GUANO model is able to reasonably model the  $\text{NH}_3$  emissions in different climate regions (Table 3), while giving better agreement with observations than any single environmental variable. Hourly measurements at the different field sites had  $R^2$  values between model and measurements of between 0.5 and 0.9 (Table 3), while  $R^2$  values with other environmental variables were generally lower.

The model-measurement comparison also illustrates how the different primary controls on  $\text{NH}_3$  emissions at the different sites. Sufficient water is needed for uric acid hydrolysis (as shown at Ascension Island), while excess water dilutes the TAN solution and is associated with increased TAN run off (Bird Island). The combined outcome of these effects is that increases in relative humidity or rain events only increase simulated  $\text{NH}_3$  emissions at arid sites such as Ascension Island (Fig. 2).

The  $\text{NH}_3$  emissions simulated by the GUANO model increased with wind speed at all sites because vertical transport and turbulent mixing of  $\text{NH}_3$  increases as aerodynamic and boundary layer resistances decrease. However, wind speed was only the major driver of  $\text{NH}_3$  emission variations at a windy site with little variation in ground temperature (Bird Island). At the other sites, ground temperature was the major driver in temporal differences of  $\text{NH}_3$  emission. Temperature is significant for two reasons: (1) it affects the rate at which uric acid converts to  $\text{NH}_3$  and (2) it affects the potential for volatilization of  $\text{NH}_3$  from the surface.

Understanding the processes behind the measured fluxes is greatly helped by considering changes in the TAN budget of the surface (Supplementary Materials Section 5) and the accumulation of TAN varied greatly between sites. The most extreme variation was found for the simulated TAN budget at Ascension Island, where rapid  $\text{NH}_3$  emission was reflected in almost complete loss of available TAN every evening. Under these circumstances,  $\text{NH}_3$  emission is primarily controlled by the uric acid hydrolysis rate, as almost all the TAN produced (unless washed-off in rain) is immediately volatilized (Fig. 2; Supplementary Material Section 2 Fig. SM 2.1). A contrasting situation was found in the simulations for Bird Island and Signy Island, where TAN production (urea hydrolysis) is much slower than at the warm sites, average TAN Production is 0.10, 0.19 and 0.06  $\text{g m}^{-2} \text{hr}^{-1}$  for Ascension Island, the Isle of May and Bird Island, respectively. Intermediate behaviour in the TAN budget was found at the Isle of May and Michaelmas Cay, with large diurnal variations, but still substantial night time values. At Michaelmas Cay, a large-scale structure in the TAN budget, varying over daily to weekly timescales was the effect of rain events on the available UA and TAN on the surface.

#### 4.2. Process-based versus empirical approaches

On a breeding season time-scale, temperature was shown to be the most influential meteorological variable, where  $\text{NH}_3$  emission

rate increases with increased temperature. Importantly this effect, which was identified empirically by Sutton et al. (2013) is here explained for the first time using a dynamic modelling approach comparing globally contrasting sites. This study therefore provides a substantial advance on initial empirical studies calculating  $\text{NH}_3$  emissions from seabirds (Wilson et al., 2004; Blackall et al., 2007), which were used to calculate  $\text{NH}_3$  emissions on a regional and country scale to Riddick et al. (2012).

The main limitation of the empirical approach of Riddick et al. (2012) was the wide uncertainty ranges related to the temperature effect and the need to constrain these by measurements, ideally using a process based approach. This is now addressed here. The GUANO model is able to explain the major differences between field sites, and the way that different variables contribute, including temperature, moisture availability and wind speed, as the most important drivers. A first application of the GUANO model reported by Sutton et al. (2013) to different sites globally showed that it was able to reproduce the main measured differences in the percentage of excreted guano that volatilizes as  $\text{NH}_3$  in relation to temperature.

The major source of uncertainty is the value for pH used in the GUANO model. Even though the same value was used at the five colonies reported in this paper, the emission estimates calculated by the GUANO model was in good agreement with emission estimates based on concentration measurements and turbulent exchange parameters. This could suggest that the biogeochemical evolution of TAN from UA and subsequent formation of  $\text{NH}_3$  happens independently of the substrate so that the pH of the underlying strata is less important. This is illustrated by the sensitivity analysis where a  $\pm 10\%$  alteration of substrate pH should equate to a sensitivity on instantaneous  $\text{NH}_3$  emission potential of +605%, –86% (i.e.  $\pm$  factor of 7). The fact that the model outcome gave a net sensitivity on simulated  $\text{NH}_3$  emissions for the Isle of May of only +73%, –22% illustrates that the amount of available TAN appears to constrain the total amount emitted and that more acid pH reduces urea hydrolysis rate (Equation SM5).

#### 4.3. $\text{NH}_3$ emissions globally

The performance of the GUANO model is illustrated for the five colony emission estimates calculated by the GUANO model shown as the  $\text{NH}_3$  emission normalized in relation to the seabird mass (Fig. 6). The GUANO model emissions are in good agreement to emission estimates based on concentration measurements and turbulent exchange parameters when they are presented with matching emissions calculated from in-situ measurements by Riddick et al. (2014, 2016) and combined with measured emissions from other sites. The additional colonies represent rock nesters on the Isle of May (Blackall et al., 2007), a cold, dry Adélie penguin colony on Antarctica (Theobald et al., 2013) and a hot dry Double-crested cormorant colony on Mullet Island, California (Tratt et al., 2013). The consistency of the observed and model estimates shows that the GUANO model could be used to calculate  $\text{NH}_3$  emissions from seabird colonies in a wide range of meteorological conditions. The GUANO model captures the large effect of  $\text{NH}_3$  emission in response to temperature and can simulate the main differences between meteorology where emission rates per unit bird body mass vary across climates by more than an order of magnitude.

It is anticipated that  $\text{NH}_3$  emissions from seabird colonies could change in a variety of ways when global climate change forecasts are considered. Changes to food supplies and changes in sea-level are both highlighted as drivers of future seabird population changes (Forcada et al., 2006; Trathan et al., 2007; Brierley, 2008). This, coupled with anticipated temperature increases in many parts of the Southern Ocean and the Antarctic Continent (Denvil, 2005),

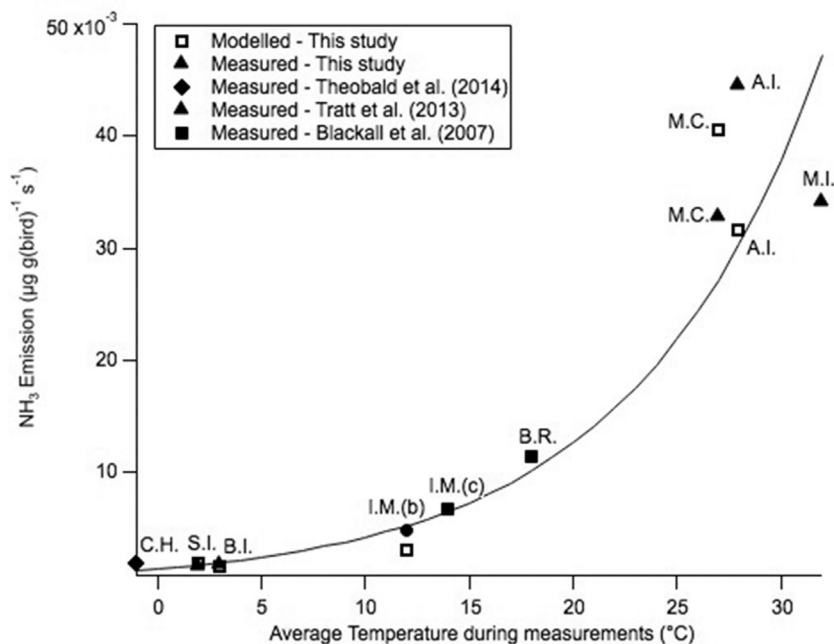


**Fig. 6.** Measured amount of excreted  $N_f$  that is volatilized as  $NH_3$  as a function of mean temperature during different field campaigns as compared with estimates of the GUANO model. The line shows the best fit of the measured data ( $NH_3$  ( $\mu\text{g g (bird)}^{-1} \text{s}^{-1}$ ) =  $0.0014e^{0.1099T}$ ;  $R^2 = 0.96$ ). The field site codes are: C.H., Cape Hallett, Antarctica; S.I., Signy Island; B.I., Bird Island, South Georgia; I.M., Isle of May, Scotland, (b) – burrows, (c) – cliffs; B.R., Bass Rock, Scotland; M.C., Michaelmas Cay, Australia; A.I., Ascension Island; M.I., Mullet Island, California.

potentially present a very different  $N_f$  landscape, associated with substantially increased  $NH_3$  emissions. Through the GUANO model we now have a quantitative tool to assess such changes in  $N_f$  partitioning which could be used to better forecast future changes to these remote nutrient-poor ecosystems.

### Acknowledgements

The work described in this paper was supported by grants from the NERC CEH Integrating Fund and the NERC thematic programme (GANE). MAS and AM gratefully acknowledge support through the EU ÉCLAIRE project. We thank the Conservation Department on Ascension Island, Queensland Department of National Parks, Recreation, Sports and Racing, Scottish National Heritage, British Antarctic Survey and Paul Hill of the University of Bangor for providing access/logistic support. We thank D. Briggs of BAS on Signy for information on meteorology and nesting penguins, and the BAS Bird Island crew for their technical and physical support (BAS CGS grant).

### Appendix A. Supplementary data

Supplementary data related to this article can be found at <http://dx.doi.org/10.1016/j.atmosenv.2017.04.020>.

### References

- Adams, P.J., Seinfeld, J.H., Koch, D., Mickley, L., Jacob, D., 2001. General circulation model assessment of direct radiative forcing by the sulfate-nitrate-ammonium-water inorganic aerosol system. *J. Geophys. Research-Atmospheres* 106 (D1), 1097–1111. <http://dx.doi.org/10.1029/2000JD900512>.
- Blackall, T.D., 2004. The Emissions of Ammonia from Seabird Colonies. PhD thesis. University of Leeds.
- Blackall, T.D., Wilson, L.J., Theobald, M.R., Milford, C., Nemitz, E., Bull, J., Bacon, P.J., Hamer, K.C., Wanless, S., Sutton, M.A., 2007. Ammonia emissions from seabird colonies. *Geophys. Res. Lett.* 34 (5), 5–17.
- Bogaard, A., Fraser, R.A., Heaton, T.H.E., Wallace, M., Vaiglava, P., Charles, M., Jones, G., Evershed, R.P., Styring, A.K., Andersen, N.H., Arbogast, R.-M., Bartosiewicz, L., Gardeisen, A., Kanstrup, M., Maier, U., Marinova, E., Ninov, L., Schäfer, M., Stephan, E., 2013. Crop manuring and intensive land management by Europe's first farmers. *Proc. Natl. Acad. Sci.* 110 (31), 12589–12594.
- Bouwman, A.F., Boumans, L.J.M., Batjes, N.H., 2002. Estimation of global  $NH_3$  volatilization loss from synthetic fertilizers and animal manure applied to arable lands and grasslands. *Glob. Biogeochem. Cycles* 16 (2). <http://dx.doi.org/10.1029/2000GB001389>, 1024.
- Brierley, A.S., 2008. Antarctic Ecosystem: are deep krill ecologica outliers or portents of a paradigm shift? *Curr. Biol.* 18, 252–254.
- Cooter, E.J., Bash, J.O., Walker, J.T., Jones, M.R., Robarge, W., 2010. Estimation of  $NH_3$  bi-directional flux from managed agricultural soils. *Atmos. Environ.* 44 (17), 2107–2115. <http://dx.doi.org/10.1016/j.atmosenv.2010.02.044>.
- Crittenden, P.D., Scrimgeour, C.S., Minnullina, G., Sutton, M.A., Tang, Y.S., Theobald, M.R., 2015. Lichen response to ammonia deposition defines the footprint of a penguin rookery. *Biogeochemistry* 122 (2), 295–311.
- Denvil, S., 2005. Intergovernmental Panel on Climate Change - Data Distribution Center. Accessed January 2016. URL was correct at a given date. <http://www.ipcc-data.org/>.
- Demmers, T.G.M., Burgess, L.R., Short, J.L., Phillips, V.R., Clark, J.A., Wathes, C.M., 1998. First experiences with methods to measure ammonia emissions from naturally ventilated cow buildings in the UK. *Atmos. Environ.* 32 (3), 285–293.
- Elliott, H.A., Collins, N.E., 1982. Factors affecting ammonia release in broiler houses. *Trans. ASAE* 25, 413.
- Elzing, A., Monteny, G.J., 1997. Ammonia emissions in a scale model of a dairy-cow house. *Trans. ASAE* 40, 713–720.
- Flechar, C.R., Massad, R.-S., Loubet, B., Personne, E., Simpson, D., Bash, J.O., Cooter, E.J., Nemitz, E., Sutton, M.A., 2013. Advances in understanding, models and parameterisations of biosphere-atmosphere ammonia exchange. *Biogeochemistry* 10, 5385–5497.
- Flesch, T.K., Wilson, J.D., Yee, E., 1995. Backward-time Lagrangian stochastic dispersion models, and their application to estimate gaseous emissions. *J. Appl. Meteorology* 34, 1320–1332.
- Forcada, J., Trathan, P.N., Reid, K., Murphy, E.J., Croxall, J.P., 2006. Contrasting population changes in sympatric penguin species in association with climate warming. *Glob. Change Biol.* 12, 411–423.
- Groot Koerkamp, P.W.G., Metz, J.H.M., Uenig, G.H., Phillips, V.R., Holden, M.R., Sneath, R.W., Short, J.L., White, R.P., Hartung, J., Seedorf, J., Schroder, M., Linkert, K.H., Pedersen, S., Takai, H., Johnsen, J.O., Wathes, C.M., 1998. Concentrations and emissions of ammonia in livestock buildings in Northern Europe. *J. Agric. Eng. Res.* 70, 79–95.
- Groot Koerkamp, P.W.G., 1994. Review on emissions of ammonia from housing systems for laying hens in relation to sources, processes, building design and manure handling. *J. Agric. Eng. Res.* 59 (2), 73–87.
- Harris, M.P., Wanless, S., 2011. *The Puffin*. T. & A.D. Poyser, London, 256.
- Massad, R.-S., Nemitz, E., Sutton, M.A., 2010. Review and parameterisation of bi-directional ammonia exchange between vegetation and the atmosphere.

- Atmos. Chem. Phys. 10, 10359–10386.
- Nemitz, E., Sutton, M.A., Schjoerring, J.K., Husted, S., Wyers, G.P., 2000. Resistance modelling of ammonia exchange over oilseed rape. *Agric. For. Meteorology* 105, 405–425.
- Nemitz, E., Milford, C., Sutton, M.A., 2001. A two-layer canopy compensation point model for describing bi-directional biosphere-atmosphere exchange of ammonia. *Q. J. R. Meteorological Soc.* 127, 815–833.
- Potter, P., Ramankutty, N., Bennett, E.M., Donner, S.D., 2010. Characterizing the spatial patterns of global fertilizer application and manure production. *Earth Interact.* 14 <http://dx.doi.org/10.1175/2009EI288.1>, 2.
- Riddick, S.N., Dragosits, U., Blackall, T.D., Daunt, F., Wanless, S., Sutton, M.A., 2012. The global distribution of ammonia emissions from seabird colonies. *Atmos. Environ.* 55, 319–327. <http://dx.doi.org/10.1016/j.atmosenv.2012.02.052>.
- Riddick, S.N., Dragosits, U., Blackall, T.D., Daunt, F., Braban, C.F., Tang, Y.S., MacFarlane, W., Taylor, S., Wanless, S., Sutton, M.A., 2014. Measurement of ammonia emissions from tropical seabird colonies. *Atmos. Environ.* 89, 35–42. <http://dx.doi.org/10.1016/j.atmosenv.2014.02.012>.
- Riddick, S.N., Dragosits, U., Blackall, T.D., Daunt, F., Braban, C.F., Tang, Y.S., Newell, M., Schmale, J., Hill, P.W., Wanless, S., Sutton, M.A., 2016. Measurement of ammonia emissions from temperate and polar seabird colonies. *Atmos. Environ.* <http://dx.doi.org/10.1016/j.atmosenv.2016.03.016>.
- Seinfeld, J.H., Pandis, S.N., 2006. *Atmospheric Chemistry and Physics: from Air Pollution to Climate Change* London. John Wiley & Sons.
- Sommer, S.G., Christensen, B.T., 1991. Effect of dry matter content on ammonia loss from surface applied cattle slurry. In: Neilsen, V.C., Voorburg, J.H., L'Hermite, P. (Eds.), *Odour and Ammonia Emissions from Livestock Farming*. Elsevier, London, UK, pp. 141–147.
- Sommer, S.G., Olesen, J.E., 2000. Modelling ammonia volatilization from animal slurry applied with trail hoses to cereals. *Atmos. Environ.* 34, 2361–2372.
- Sutton, M.A., Asman, W.A.H., Ellerman, T., van Jaarsveld, J.A., Acker, K., Aneja, V., Duyzer, J.H., Horvath, L., Paramonov, S., Mitosinkova, M., Tang, Y.S., Achermann, B., Gauger, T., Bartnicki, J., Neftel, A., Erismann, J.W., 2003. Establishing the link between ammonia emission control and measurements of reduced nitrogen concentrations and deposition. *Environ. Monit. Assess.* 82 (2), 149–185.
- Sutton, M.A., Fowler, D., Moncrieff, J.B., 1993. The exchange of atmospheric ammonia with vegetated surfaces. 1. Unfertilized vegetation. *Q. J. R. Meteorological Soc.* 119, 1023–1045.
- Sutton, M.A., Burkhardt, J.K., Guerin, D., Nemitz, E., Fowler, D., 1998. Development of resistance models to describe measurements of bi-directional ammonia surface atmosphere exchange. *Atmos. Environ.* 32 (3), 473–480.
- Sutton, M.A., Reis, S., Billen, G., Cellier, P., Erismann, J.W., Mosier, A.R., Nemitz, E., Sprent, J., van Grinsven, H., Voss, M., Beier, C., Skiba, U., 2012. "Nitrogen & global change" preface. *Biogeosciences* 9 (5), 1691–1693. <http://dx.doi.org/10.5194/bg-9-1691-2012>.
- Sutton, M.A., Reis, S., Riddick, S.N., Dragosits, U., Nemitz, E., Theobald, M.R., Tang, Y.S., Braban, C.F., Vieno, M., Dore, A.J., Mitchell, R.F., Wanless, S., Daunt, F., Fowler, D., Blackall, T.D., Milford, C., Flechard, C.R., Loubet, B., Massad, R., Cellier, P., Personne, E., Coheur, P.F., Clarisse, L., Van Damme, M., Ngadi, Y., Clerbaux, C., Skjoth, C.A., Geels, C., Hertel, O., Kruit, R.J.W., Pinder, R.W., Bash, J.O., Walker, J.T., Simpson, D., Horvath, L., Misselbrook, T.H., Bleeker, A., Dentener, F., de Vries, W., 2013. Towards a climate-dependent paradigm of ammonia emission and deposition. *Philosophical Trans. R. Soc. B-Biological Sci.* 368, 20130166.
- Tang, Y.S., Cape, J.N., Sutton, M.A., 2001. Development and types of passive samplers for NH<sub>3</sub> and NO<sub>x</sub>. In proceedings of the international symposium on passive sampling of gaseous pollutants in ecological research. *Sci. World* 1, 513–529.
- Theobald, M.R., Crittenden, P.D., Tang, Y.S., Sutton, M.A., 2013. The application of inverse-dispersion and gradient methods to estimate ammonia emissions from a penguin colony. *Atmos. Environ.* 81, 320–329.
- Trathan, P.N., Forcada, J., Murphy, E.J., 2007. Environmental forcing and Southern Ocean marine predator populations: effects of climate change and variability. *Philosophical Trans. R. Soc. B-Biological Sci.* 362, 2351–2365.
- Tratt, D., M., Buckland, K.N., Young, S.J., Johnson, P.D., Riesz, K.A., Molina, K.C., 2013. Remote sensing visualization and quantification of ammonia emission from an inland seabird colony. *J. Appl. Remote Sens.* 7 (1), 073475.
- Wentworth, G.R., Murphy, J.G., Croft, B., Martin, R.V., Pierce, J.R., Côté, J.-S., Courchesne, I., Tremblay, J.-É., Gagnon, J., Thomas, J.L., Sharma, S., Toom-Saunty, D., Chivulescu, A., Levasseur, M., Abbatt, J.P.D., 2015. Ammonia in the summertime Arctic marine boundary layer: sources, sinks and implications. *Atmos. Chem. Phys. Discuss.* 15, 29973–30016. <http://dx.doi.org/10.5194/acpd-15-29973-2015>.
- Wilson, L.J., Bacon, P.J., Bull, J., Dragosits, U., Blackall, T.D., Dunn, T.E., Hamer, K.C., Sutton, M.A., Wanless, S., 2004. Modelling the spatial distribution of ammonia emissions from seabirds in the UK. *Environ. Pollut.* 131, 173–185.
- Zhu, R.B., Sun, J.J., Liu, Y.S., Gong, Z.J., Sun, L.G., 2011. Potential ammonia emissions from penguin guano, ornithogenic soils and seal colony soils in coastal Antarctica: effects of freezing-thawing cycles and selected environmental variables. *Antarct. Sci.* 23, 78–92.